Pressure-induced structural transition of $Cd_xZn_{1-x}O$ alloys

Yabin Chen,[1,a)] Shuai Zhang,[2,a)] Weiwei Gao,[3] Feng Ke,[4] Jinyuan Yan,[5] Bivas Saha,[1] Changhyun Ko,[1] Joonki Suh,[1] Bin Chen,[4] Joel W. Ager III,[1,3] Wladek Walukiewicz,[3] Raymond Jeanloz,[2] and Junqiao Wu[1,3,b)]
[1]*Department of Materials Science and Engineering, University of California, Berkeley, California 94720, USA*
[2]*Department of Earth and Planetary Science, University of California, Berkeley, California 94720, USA*
[3]*Materials Sciences Division, Lawrence Berkeley National Laboratory, Berkeley, California 94720, USA*
[4]*Center for High Pressure Science and Technology Advanced Research, Shanghai 201203, China*
[5]*Advanced Light Source, Lawrence Berkeley National Lab, Berkeley, California 94720, USA*

(Received 8 February 2016; accepted 5 April 2016; published online 13 April 2016)

$Cd_xZn_{1-x}O$ alloys, as a transparent conducting oxide, have recently attracted much attention for potential optoelectronic applications. In this letter, we report a hydrostatic pressure-induced phase transition of $Cd_xZn_{1-x}O$ alloys from the wurtzite to the rocksalt structure and its phase diagram probed using a diamond anvil cell. It is found that the transition pressure, determined by changes in optical and structural properties, depends sensitively on the composition. As the Cd content increases, the critical pressure decreases, until at $x = 0.67$ where the alloy is intrinsically stable in the rocksalt phase even at ambient pressure. The wurtzite phase is light emitting with a direct bandgap that slightly widens with increasing pressure, while the rocksalt phase has a much wider bandgap that is indirect. The pressure-sensitive light emission and phase transition may find potential applications in fields such as stress sensing and energy storage. *Published by AIP Publishing.*
[http://dx.doi.org/10.1063/1.4947022]

At ambient condition, ZnO takes the wurtzite crystal structure and it is a brightly light-emitting semiconductor with a direct bandgap (E_g) of 3.3 eV.[1,2] The high luminescence efficiency and piezoelectricity of ZnO have rendered it a candidate material for light emitting diodes[2–4] and mechanical energy harvesting devices.[5] Upon the application of hydrostatic pressure of ~9 GPa, ZnO transforms into the rocksalt structure, which has an indirect E_g of ~2.4 eV and a direct gap of ~4.6 eV.[6,7] In contrast, CdO is inherently a rocksalt-structured semiconductor with an indirect E_g of ~2.3 eV and high free electron density arising from native defects.[8,9] Uniformly mixing CdO with ZnO leads to a random alloy of $Cd_xZn_{1-x}O$.[10] At $x \lesssim 0.67$, $Cd_xZn_{1-x}O$ has the wurtzite crystal structure, with a direct E_g ranging from 1.6 to 3.3 eV covering the entire visible spectrum.[9] The alloys in this composition range typically have a high free electron density ranging from mid-10^{19} to $>10^{20}$ cm^{-3} and a respective electron mobility of ~20 cm^2 V^{-1} s^{-1}. These properties make $Cd_xZn_{1-x}O$ a promising candidate for key materials in light emission, transparent conducting, or photovoltaic applications.[1,2,11]

As CdO is rocksalt structured, it is not surprising that the stable crystal structure of $Cd_xZn_{1-x}O$ at ambient conditions becomes rocksalt as x becomes large ($\gtrsim$0.67).[9] The accompanying abrupt opening in E_g, increase in electron mobility, and quenching of light emission efficiency at this composition link the structural transition to wide modulation of the electronic properties. As a result, the $Cd_xZn_{1-x}O$ alloy system becomes attractive and relevant for potential applications with the benefit of the phase transition. In this work, we explore the wurtzite-rocksalt structural transition of $Cd_xZn_{1-x}O$ in response to the application of hydrostatic pressure, as opposed to variation in chemical composition. The diamond anvil cell (DAC) offers a powerful means of modulating structural phase transitions and the accompanying physical properties of semiconductors.[12–14] By investigating the light emission, optical absorption, and x-ray diffraction (XRD) of the $Cd_xZn_{1-x}O$ alloys with a range of compositions using a DAC, we construct a composition (x) – pressure (P) diagram of $Cd_xZn_{1-x}O$. Moreover, density functional theory (DFT) calculations show that the phase transition is primarily attributed to volume deformation as opposed to a reduction in internal energy. Our results establish the physical picture behind the phase stability and transition of the $Cd_xZn_{1-x}O$ system for potential technological applications.[1,2,15]

$Cd_xZn_{1-x}O$ alloys were grown on soda lime glass using a dual-source radio frequency magnetron sputtering system with separate CdO and ZnO targets. The chamber was evacuated to 1×10^{-6} Torr prior to deposition. The background pressure was maintained at ~5 mTorr of Ar at a substrate temperature of 270 °C during the deposition. The composition of alloys was controlled by varying the sputtering power and substrate-to-target distance of the CdO and ZnO targets. Film stoichiometry and thickness of each sample were determined by the Rutherford backscattering technique. The obtained film thicknesses range from 98 to 275 nm.

Hydrostatic pressures were applied by a symmetric DAC with 300 μm culet size. The stainless-steel foil used as gasket material was indented to a depth of ~30 μm, after which a hole was laser-drilled to form the sample chamber. The pressure transmission medium was a 4:1 mixture of methanol and ethanol, and pressure was calibrated by the photoluminescence

[a)]Y. Chen and S. Zhang contributed equally to this work.
[b)]Author to whom correspondence should be addressed. Electronic mail: wuj@berkeley.edu.

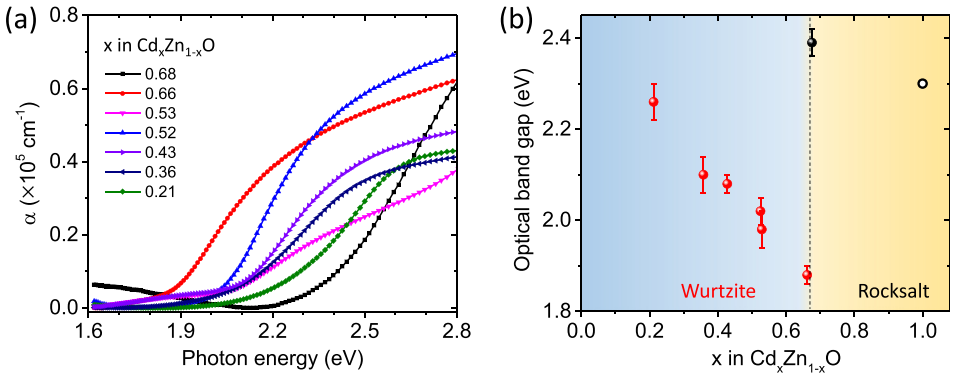

FIG. 1. (a) Optical absorption coefficients of the as-grown $Cd_xZn_{1-x}O$ alloys; (b) optical bandgap of $Cd_xZn_{1-x}O$ alloys determined from the absorption curves. The open circle in (b) represents E_g of CdO ($x = 1.0$) from Ref. 9.

(PL) wavelength of ruby. The glass substrate coated with the film was polished down to a thickness of $<20\ \mu$m before loading into the DAC. Optical transmission was measured with a home-made spectrometer system equipped with a tungsten halogen lamp as the light source and a photo-multiplier tube as the detector. PL spectra were obtained using a 488 nm laser as the excitation source. Synchrotron XRD measurements were performed at Beamline12.2.2 of the Advanced Light Source (ALS), Lawrence Berkeley National Laboratory. The beam energy was 18 keV ($\lambda = 0.6888$ Å), and the XRD signal was collected with a MAR345 image plate.

First-principles calculations were performed using the Perdew-Burke-Ernzerhof[16] exchange-correlation functional and the projector augmented wave method[17] as implemented in the Vienna *ab-initio* Simulation Package.[18,19] The Cd ($4d^{10}5s^2$), Zn ($3d^{10}4s^2$), and O ($2s^22p^4$) were treated as the valence electrons. The core radii in the pseudopotentials were 2.3, 2.3, and 1.52 Bohr for Cd, Zn, and O, respectively. We used $2 \times 2 \times 1$ and $2 \times 2 \times 2$ supercells for the wurtzite and rocksalt phases, respectively, and randomly substitute corresponding number of Zn by Cd to construct $Cd_xZn_{1-x}O$ alloys. We relaxed the supercells using a cutoff energy of 550 eV and Γ-centered Monkhorst-Pack[20,21] k-mesh of $4 \times 4 \times 4$ or $8 \times 8 \times 8$ for the rocksalt or the wurtzite structure, respectively, until the force on each atom was smaller than 0.02 eV/Å. Starting from the relaxed structures, follow-up calculations using 800 eV cutoff energy and $6 \times 6 \times 6$ or $10 \times 10 \times 10$ k-mesh were used for the rocksalt or wurtzite structure, respectively, to determine the energy more precisely. Tests showed that using these settings the energy converged to within 10^{-4} eV/formula unit (f.u.).

Figure 1(a) shows the optical absorption coefficients (α) of $Cd_xZn_{1-x}O$ alloys with representative compositions. A clear onset can be identified on these absorption curves, which was used to extract the optical E_g of these materials.[6,22] The E_g that we obtained as a function of Cd concentration (x) is consistent within error with the data reported in Ref. 9 (Fig. 1(b)). In the wurtzite structure ($x < 0.67$), E_g rapidly decreases with x from $E_g = 3.3$ eV for ZnO toward a hypothetical E_g of ∼ 1.4 eV for wurtzite CdO (wurtzite CdO has not been experimentally synthesized). At x ∼0.67, however, E_g abruptly increases from ∼1.9 to ∼2.4 eV, due to the wurtzite-rocksalt transition near this composition. As thermodynamics implies that pressure drives the structural transition from the wurtzite to the denser rocksalt structure, our study focused on compressing alloys with $x < 0.67$ that are initially in the wurtzite structure.

Figure 2 shows the pressure behavior of a $Cd_xZn_{1-x}O$ alloy at the composition of $x = 0.66$. The wurtzite alloys all exhibit bright PL at ambient pressure as shown in Fig. 2(a). Upon the application of hydrostatic pressure, however, the PL intensity is rapidly suppressed and eventually quenched at a threshold pressure, P_c. To probe the E_g near and above P_c, we measured optical absorption of the films inside the DAC gasket chamber, as shown in Fig. 2(b). The E_g determined from both PL and absorption spectra is plotted as functions of pressure in Fig. 2(c). It can be seen that in the wurtzite phase when $P < P_c$, E_g slightly increases with pressure, with a weak pressure coefficient of $dE_g/dP \sim 22$ meV/GPa. The fact that, as shown in Fig. 2(a), the PL intensity is reduced gradually rather than abruptly at P_c, indicates an inhomogeneous transition, which may be caused by the

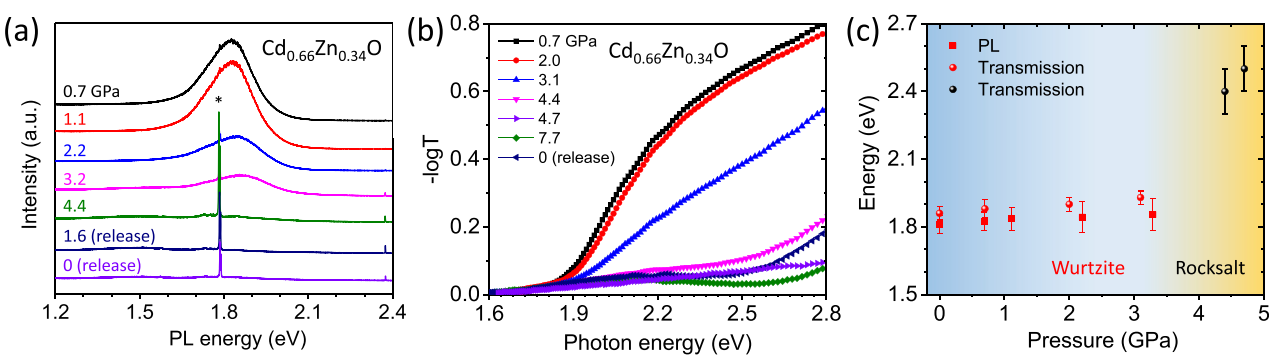

FIG. 2. Pressure dependence of PL (a) and transmission (b) spectra of $Cd_{0.66}Zn_{0.34}O$. Absorption edge energy and PL peak energy as a function of DAC pressure are shown in (c). The asterisk in (a) indicates the ruby luminescence peak. All data were measured during the pressure loading process unless labeled with "release," which indicates measurements during the pressure releasing process.

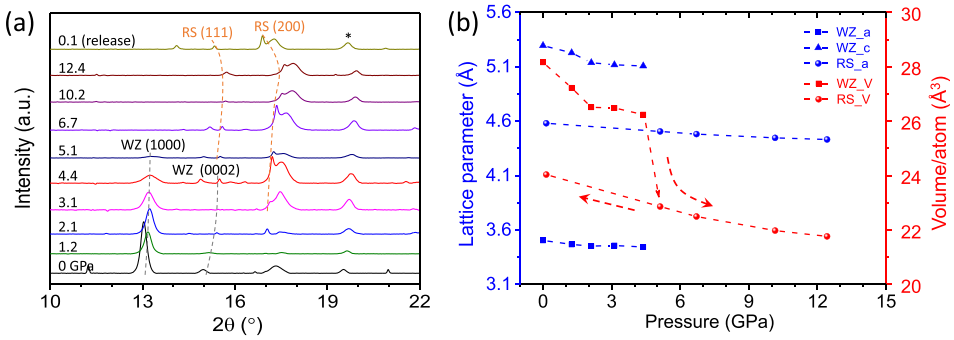

FIG. 3. Phase transition of $Cd_{0.66}Zn_{0.34}O$ determined by synchrotron XRD. XRD curves (a) of $Cd_{0.66}Zn_{0.34}O$, and its extracted lattice parameters and volume (b) at different pressures. The asterisk in (a) indicates the peak from the gasket. WZ and RS indicate wurtzite and rocksalt structures, respectively.

polycrystalline nature of these alloy films. It is interesting to note that after releasing the pressure, the new phase persists, indicating that the phase transition is irreversible, or with a wide hysteresis that extends down to ambient pressure. Similar effects have also been reported for the intrinsic ZnO under high pressures[13,23] and were attributed to kinetic barriers existing in such polycrystalline films that would hinder the system from transitioning back to the wurtzite structure.

To further investigate the pressure induced evolution of the crystallographic structure of the $Cd_xZn_{1-x}O$ alloys, *in situ* micro-XRD measurements were carried out.[24,25] The XRD patterns of $Cd_{0.66}Zn_{0.34}O$ after background subtraction are shown in Fig. 3(a). Based on the characteristic peaks, the low-pressure phase can be clearly indexed to a wurtzite structure. The wurtzite XRD peaks gradually lose their intensity and disappear at $P_c \sim 4.0$ GPa. We note that the peak position of WZ (0002) in low pressure range ($P < 4$ GPa) is very close to that of RS (111) under high pressure ($P > 4$ GPa). Importantly, the strongest WZ (1000) peak completely disappears when $P > 5.1$ GPa, defining P_c for the structural phase transition. At $P > P_c$, the material transforms into a rocksalt structure, with several new weak peaks indexed as the rocksalt (111) and (200) planes.

The irreversibility of the pressure-induced phase transition is confirmed by the XRD data: after pressure is released, the rocksalt structure persists even at ambient pressure. This effect indicates that the rocksalt structure can be kinetically stabilized at ambient pressure, and we interpret the wurtzite-rocksalt transition as a first-order transition with a wide hysteresis. This effect will be further analyzed in conjunction with the DFT calculation in a later part of the article. We further calculated the lattice constants and specific volume of the alloy and plotted them as a function of pressure in Fig. 3(b). It can be seen that a large volume collapse, a 15.4% reduction in volume, occurs at P_c.

Figure 4(a) shows the x-P phase diagram of the $Cd_xZn_{1-x}O$ alloys obtained from our high pressure experiments as well as previously reported P_c of ZnO.[9,22] It can be seen that the threshold pressure P_C decreases monotonically as x increases, defining a concave phase boundary between the wurtzite and rocksalt phases of the alloys. In order to understand the phase relations, we have carried out first-principles calculations on the energies of the two phases at two different compositions, $x = 0.625$ and $x = 0.25$. The results are shown in Fig. 4(b). As the pressure increases to P_C, the enthalpy of the rocksalt phase becomes lower than that of the wurtzite phase (i.e., $\Delta H < 0$); the transition pressure P_c is 8.84 GPa for $x = 0.25$, and it decreases to 4.37 GPa for $x = 0.625$. These findings agree with those determined in our experiments. The enthalpy difference ΔH can be decomposed into an internal energy difference ΔU and the pressure term $\Delta(PV)$. ΔU represents effects of bonding in the crystal and is positive and nearly independent of pressure, which acts as an energy barrier to stabilize the wurtzite phase. As the pressure increases, phase transition occurs when this energy barrier is overcome by $\Delta(PV)$, which becomes more negative with pressure because of the smaller volume of the rocksalt phase. When the Cd fraction is higher, increasing amount of electrons occupy the deeper Cd-d states of the rocksalt phase, which decreases ΔU, lowers the barrier and eases the transition. When x exceeds ~0.7, ΔU itself becomes negative, which stabilizes the rocksalt phase even at ambient condition.

At thermodynamic equilibrium, phase separation may occur associated with the wurtzite-rocksalt transformation for $Cd_xZn_{1-x}O$ alloys with $x < 0.67$, akin to that observed in alkali halides.[26–28] We did not find evidence for the phase loop resulting from such separation, but this is consistent with the kinetic hindrance we observed for the structural transformation itself. That is, separation (e.g., by diffusion)

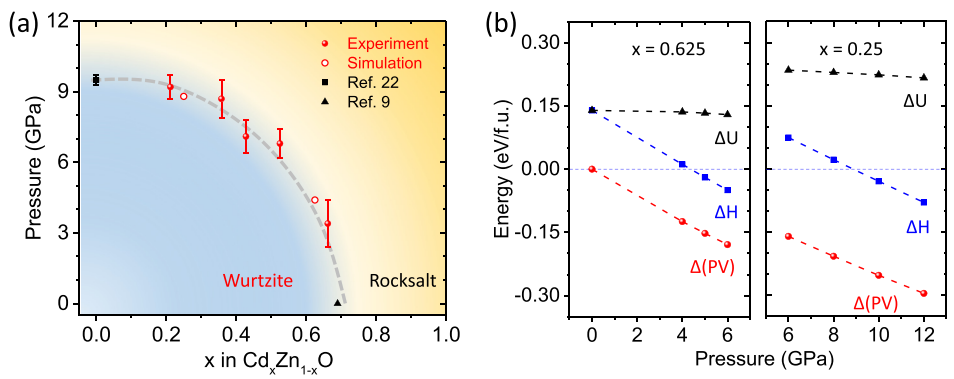

FIG. 4. (a) x-P phase diagram of $Cd_xZn_{1-x}O$ alloys. The dashed gray line is drawn to guide the eye. (b) Calculated energies of the rocksalt phase relative to the wurtzite phase of $Cd_{0.625}Zn_{0.375}O$ (left) and $Cd_{0.25}Zn_{0.75}O$ (right).

into separate phases having distinct composition is likely less feasible at room temperature, at least over the timescales of our experiments, than the local atomic rearrangement associated with the wurtzite-rocksalt coordination change. Therefore, our experiments likely document a compositionally frozen metastable equilibrium between the two crystal structures. The result is that intermediate compositions of the alloy in the high-pressure rocksalt phase can be quenched to zero pressure.

In conclusion, we have mapped out the composition-pressure phase diagram of $Cd_xZn_{1-x}O$ alloys using a DAC in conjunction with characterization techniques of PL, optical absorption, and synchrotron XRD. A concave phase boundary is established between the light-emitting, wurtzite phase at low pressures and the wide-bandgap, rocksalt phase at high pressures. The phase transition is first-order with a wide hysteresis such that the induced phase persists when the pressure is released to ambient conditions. Namely, the pressure effect is non-volatile within the conditions of our experiments. As the pressure-driven transition is accompanied with drastic modification of electronic and optical functionalities, potential applications of these alloys may be envisioned in fields such as stress sensing, light emission, actuation,[29] and thermal/mechanical energy storage.[30]

This work was supported by the Electronic Materials Program at the Lawrence Berkeley National Laboratory, which is supported by the Office of Science, Office of Basic Energy Sciences, of the U.S. Department of Energy under Contract No. DE-AC02-05CH11231. J.W., J.W.A., and Y.C. acknowledge support from the Singapore-Berkeley Research Initiative for Sustainable Energy (SinBeRISE). The laser milling was supported by COMPRES (Grant No. EAR 11-57758). S.Z. was supported in part by the U.S. Department of Energy, Grant No. DE-SC0010517. Y.C. thanks Dr. F. B. Tian (Jilin University, China) for his helpful discussion on DFT simulations.

[1]A. Janotti and C. G. Van de Walle, Rep. Prog. Phys. **72**, 126501 (2009).
[2]U. Ozgur, Y. I. Alivov, C. Liu, A. Teke, M. A. Reshchikov, S. Dogan, V. Avrutin, S. J. Cho, and H. Morkoc, J. Appl. Phys. **98**, 41301 (2005).
[3]M. H. Huang, S. Mao, H. Feick, H. Q. Yan, Y. Y. Wu, H. Kind, E. Weber, R. Russo, and P. D. Yang, Science **292**, 1897 (2001).
[4]A. Tsukazaki, A. Ohtomo, T. Onuma, M. Ohtani, T. Makino, M. Sumiya, K. Ohtani, S. F. Chichibu, S. Fuke, Y. Segawa, H. Ohno, H. Koinuma, and M. Kawasaki, Nat. Mater. **4**, 42 (2005).
[5]Z. L. Wang, J. Phys.: Condens. Matter **16**, R829 (2004).
[6]J. A. Sans, A. Segura, F. J. Manjon, B. Mari, A. Munoz, and M. J. Herrera-Cabrera, Microelectron. J. **36**, 928 (2005).
[7]A. N. Baranov, P. S. Sokolov, V. A. Tafeenko, C. Lathe, Y. V. Zubavichus, A. A. Veligzhanin, M. V. Chukichev, and V. L. Solozhenko, Chem. Mater. **25**, 1775 (2013).
[8]D. M. Detert, K. B. Tom, C. Battaglia, J. D. Denlinger, S. H. N. Lim, A. Javey, A. Anders, O. D. Dubon, K. M. Yu, and W. Walukiewicz, J. Appl. Phys. **115**, 233708 (2014).
[9]D. M. Detert, S. H. M. Lim, K. Tom, A. V. Luce, A. Anders, O. D. Dubon, K. M. Yu, and W. Walukiewicz, Appl. Phys. Lett. **102**, 232103 (2013).
[10]T. Makino, Y. Segawa, M. Kawasaki, A. Ohtomo, R. Shiroki, K. Tamura, T. Yasuda, and H. Koinuma, Appl. Phys. Lett. **78**, 1237 (2001).
[11]W. Z. Wu, X. N. Wen, and Z. L. Wang, Science **340**, 952 (2013).
[12]F. Decremps, J. Pellicer-Porres, A. M. Saitta, J. C. Chervin, and A. Polian, Phys. Rev. B **65**, 92101 (2002).
[13]W. Shan, W. Walukiewicz, J. W. Ager, K. M. Yu, Y. Zhang, S. S. Mao, R. Kling, C. Kirchner, and A. Waag, Appl. Phys. Lett. **86**, 153117 (2005).
[14]X. J. Sha, F. B. Tian, D. Li, D. F. Duan, B. H. Chu, Y. X. Liu, B. B. Liu, and T. Cui, Sci. Rep. **5**, 11003 (2015).
[15]C. F. Pan, L. Dong, G. Zhu, S. M. Niu, R. M. Yu, Q. Yang, Y. Liu, and Z. L. Wang, Nat. Photonics **7**, 752 (2013).
[16]J. P. Perdew, K. Burke, and M. Ernzerhof, Phys. Rev. Lett. **77**, 3865 (1996).
[17]G. Kresse and D. Joubert, Phys. Rev. B **59**, 1758 (1999).
[18]G. Kresse and J. Furthmuller, Comput. Mater. Sci. **6**, 15 (1996).
[19]G. Kresse and J. Furthmuller, Phys. Rev. B **54**, 11169 (1996).
[20]H. J. Monkhorst and J. D. Pack, Phys. Rev. B **13**, 5188 (1976).
[21]J. D. Pack and H. J. Monkhorst, Phys. Rev. B **16**, 1748 (1977).
[22]A. Segura, J. A. Sans, F. J. Manjon, A. Munoz, and M. J. Herrera-Cabrera, Appl. Phys. Lett. **83**, 278 (2003).
[23]Z. H. Dong, K. K. Zhuravlev, S. A. Morin, L. S. Li, S. Jin, and Y. Song, J. Phys. Chem. C **116**, 2102 (2012).
[24]C. M. Lin, K. L. Lin, Y. K. Chern, C. H. Hsu, H. S. Sheu, Y. F. Liao, Y. W. Suen, S. R. Jian, and J. Y. Juang, J. Alloys Compd. **604**, 298 (2014).
[25]H. Z. Liu, Y. Ding, M. Somayazulu, J. Qian, J. Shu, D. Hausermann, and H. K. Mao, Phys. Rev. B **71**, 212103 (2005).
[26]P. Bhardwaj and S. Singh, Cent. Eur. J. Chem. **10**, 1391 (2012).
[27]N. V. C. Shekar and K. G. Rajan, Bull. Mater. Sci. **24**, 1 (2001).
[28]X. Y. Li and R. Jeanloz, Phys. Rev. B **36**, 474 (1987).
[29]K. Liu, C. Cheng, Z. T. Cheng, K. V. Wang, R. Ramesh, and J. Q. Wu, Nano Lett. **12**, 6302 (2012).
[30]H. Tokoro, M. Yoshikiyo, K. Imoto, A. Namai, T. Nasu, K. Nakagawa, N. Ozaki, F. Hakoe, K. Tanaka, K. Chiba, R. Makiura, K. Prassides, and S. Ohkoshi, Nat. Commun. **6**, 7037 (2015).